

# **Light Induced Electron Transfer Processes in Surface Engineered Eco-friendly CuInS<sub>2</sub> Quantum Dots**



*A thesis submitted towards partial fulfilment  
of BS-MS Dual Degree Programme*

**By**

**Jewel Ann Maria Xavier  
20131073**


**Under the guidance of**

**Dr. Pramod P. Pillai**

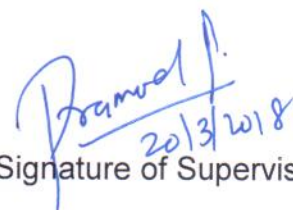
Assistant Professor, Department of Chemistry  
Indian Institute of Science Education and Research,  
Pune

## Certificate

This is to certify that this dissertation titled '**Light Induced Electron Transfer Processes in Surface Engineered Eco-friendly CuInS<sub>2</sub> Quantum Dots**' towards the partial fulfilment of the BS-MS dual degree programme at the Indian Institute of Science Education and Research, Pune represents study/work carried out by **Jewel Ann Maria Xavier** at **IISER, Pune** under the supervision of **Dr. Pramod P. Pillai**, Assistant Professor, Department of Chemistry during the academic year, **2017-2018**.



Signature of Student



Signature of Supervisor

Date: *20/3/2018*

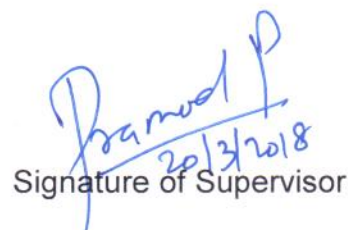
Place: *Pune*

## Declaration

I hereby declare that the matter embodied in the report titled '**Light Induced Electron Transfer Processes in Surface Engineered Eco-friendly CuInS<sub>2</sub> Quantum Dots**' are the results of the work carried out by me at the Department of Chemistry, IISER, Pune, under the supervision of Dr. Pramod P. Pillai and the same has not been submitted elsewhere for any other degree.



Signature of Student



Signature of Supervisor

Date: 20/3/2018

Place: Pune

## *Acknowledgement*

Research is never a one man show and I would like to acknowledge my army, without whom this thesis would not have been made possible.

Firstly, I would like to express my sincere gratitude to Dr. Pramod P. Pillai who has been my mentor for the past two years for his guidance and insights. He has been a constant pillar of support throughout my research, giving his valuable suggestions and directions when in need. Discussions with him have always given me newer and broader perspectives, be it in terms of research or future plans. He was always there and free to approach. I am very grateful to have had an opportunity to work and be guided by such a person. I would also like to take this opportunity to thank Dr. Angshuman Nag who has been kind enough to be my TAC member and for his valuable suggestions.

A person who has been an integral part of my research. I would like to thank Ms. Devatha Gayathri for all her directions and help without whom I would not have been to complete this herculean task. She has always guided and supported me whenever I faced a hurdle. I would like to thank all my lab members, Soumendu, Anish, Sumit and Indra, for their advices and help during my research. A big thank you to all of them for creating a comfy and easy to work environment for me.

I would also like to thank IISER for providing state-of-the-art facilities and research atmosphere.

Friends are always an inexcusable part in one's life. I would like to thank Aswin, Govind, Swetha and all my other friends for being there to pull me up when I was down. They have always been there to share, be it my worries or lame jokes. I would like to thank them for always being there to count on.

The page would be incomplete without thanking my superheroes, Appa and Amma. They have always supported and stood by my decisions. Their constant concern and encouragement has helped me to be what I am. A big heartfelt thank you to them for being there. I would also like to thank all my family members for their support.

Above all, I would like to thank God Almighty for all his blessings.

## Table of Contents

<b>Abstract</b> .....	<b>7</b>
<b>1. Introduction</b> .....	<b>8</b>
<b>2. Experimental Section</b> .....	<b>10</b>
2.1. Synthesis of CIS QDs.....	10
2.2. Preparation of water soluble CIS QDs.....	11
2.3. Photoluminescence quenching Experiment.....	12
2.4. Stern-Volmer Analysis.....	12
<b>3. Instrumentation and Techniques used</b> .....	<b>13</b>
3.1. UV-vis absorption studies.....	13
3.2. Photoluminescence studies.....	13
3.3. Time resolved measurements.....	13
3.4. Zeta potential measurements.....	13
3.5. X-Ray Diffraction (XRD) measurements.....	14
3.6. High Resolution Transmission Electron Microscopy (HRTEM).....	14
<b>4. Results and Discussion</b> .....	<b>14</b>
4.1. Characterization of CIS QDs.....	14
4.2. Photoluminescence quenching studies.....	16
4.3. Proof for photoinduced electron transfer.....	19
4.3.1. Comparison of photoluminescence quenching studies in ambient and inert conditions.....	19
4.3.2. Effect of solvent polarity on photoluminescence quenching studies.....	20
4.3.3. Effect of temperature on photoluminescence quenching studies.....	23
4.4. Mode of interaction between CIS QD donor and ICG acceptor molecules..	24
4.4.1. Reduction in electrostatic attraction.....	24
4.4.2. Photoinduced electron transfer in organic solvent.....	26
4.5. Photoinduced electron transfer between [-] CIS QD and [+] Methylene blue dye.....	27
4.5.1. Photoluminescence quenching studies.....	29
4.5.2. Demonstrating the role of electrostatics in CIS QD-MB nanohybrid.....	30
<b>5. Conclusions and future directions</b> .....	<b>32</b>
<b>References</b> .....	<b>33</b>

## List of Figures

4.1. Spectroscopic and microscopic characterization of water soluble CIS QDs.....	15
4.2. Characterization of ICG dye molecule.....	16
4.3. Condition for plausible energy and electron transfer processes.....	17
4.4. Photoluminescence studies in [+] CIS QD- [-] ICG dye.....	18
4.5. PL quenching studies in ambient and inert conditions.....	20
4.6. Effect of solvent polarity on PL quenching.....	22
4.7. Effect of temperature on PL quenching.....	23
4.8. PET between [-] CIS QDs and [-] ICG dye.....	25
4.9. PET in organic solvent, CHCl <sub>3</sub> .....	27
4.10. Characterization of methylene blue (MB) dye .....	28
4.11. Condition for plausible energy and electron transfer in [-] CIS QD- [+] MB dye nanohybrid.....	28
4.12. Photoluminescence quenching studies in [-] CIS QD- [+] MB nanohybrid....	30
4.13. Exclusivity of electrostatic effect in the PL quenching in [-] CIS QD- [+] MB nanohybrid.....	31

## List of Schemes

1.1. Forster Resonance Energy Transfer (FRET) and Photoinduced Electron Transfer (PET).....	8
1.2. Effect of quantum confinement.....	9
2.1. Place exchange reaction between OAm capped CIS QDs and [+] TMA/ [-] MUA ligand.....	12
4.1. Electrostatic attraction and repulsion possible between [-] CIS QDs- [-] ICG dye.....	26

## List of Tables

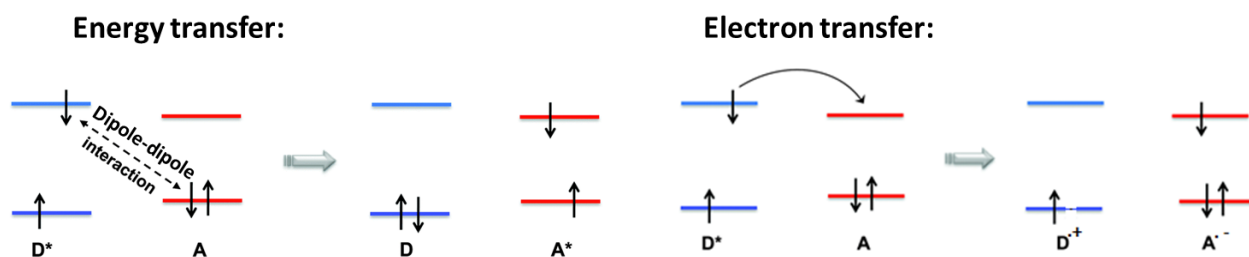
4.1. Effect of solvent polarity on PL quenching.....	20
4.2. Effect of temperature on PL quenching.....	22

## Abstract

Fundamental photophysical studies in eco-friendly as well as biocompatible quantum dots (QDs) are essential to realize the unique size dependent optoelectronic properties of QDs in practical applications. In this regard, the current thesis focuses on investigating the light harvesting properties in Copper Indium Sulphide (CuInS<sub>2</sub>) QDs. A precise surface engineering helped in imparting aqueous stability and tuning of surface charge of CuInS<sub>2</sub>/ZnS (CIS) QDs, with ~60% retention of its photoluminescence quantum yield. Further, the ability of CIS QDs to participate in light harvesting processes in aqueous medium is investigated. A light induced electron transfer in the Near Infrared (NIR) region is successfully demonstrated with CIS QDs as the donor and Indocyanine green (ICG) dye as the acceptor. The process of electron transfer was confirmed by carrying out quenching experiments under (i) Ar atmosphere, (ii) varying temperature and (iii) different solvent polarity. The efficiency of electron transfer was estimated to be as high as 85 % in aqueous medium, which is attributed to the strong electrostatic attraction between cationic CIS QD and anionic ICG dye. The use of CIS QDs as an efficient electron donor was extended towards methylene blue acceptor dye as well. Our studies help in expanding the scope of eco-friendly CuInS<sub>2</sub> QDs beyond organic solvents, thereby enabling its future potential use in both optoelectronic and biomedical applications.

## 1. Introduction

Understanding the ‘*nature*’ has been of prime importance for mankind from time immemorial. Researchers have worked relentlessly to get deeper insight on the diverse processes occurring in nature. Of these, light induced processes pertain to a class of its own. Over the years, vast research has been carried out centered on light induced processes, specifically energy and electron transfer. “*How to mimic photosynthesis?*” is considered as a golden question of the era. Even a complex process such as photosynthesis when examined closely reveals an ensemble of fundamental light induced processes, namely Forster Resonance Energy Transfer (FRET) and Photoinduced Electron Transfer (PET).<sup>1,2</sup> FRET is a light induced process that operates through long range dipole-dipole interaction via a non-radiative transfer of energy from a photoexcited donor to an acceptor in the ground state (**Scheme 1.1**).<sup>3</sup> FRET finds its application in a range of fields, from energy devices to biological rulers.<sup>4,5</sup> Photoinduced Electron Transfer (PET) involves the transfer of an electron from a photoexcited state of the donor to the acceptor, resulting in transient redox species.<sup>6</sup> PET also possesses a wide range of applicability especially in device fabrication and photosynthesis mimetics.<sup>1,7</sup>

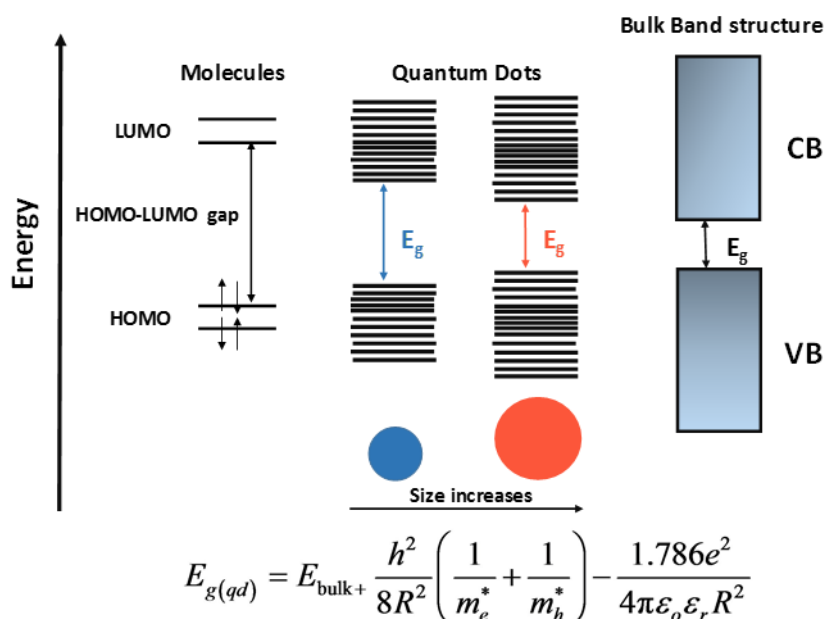


**Scheme 1.1:** A schematic representation of Forster Resonance Energy Transfer (FRET) and Photoinduced Electron Transfer (PET).<sup>8</sup> (Adapted from ref. 8)

An ideal candidate for FRET and PET studies should possess a high absorption coefficient, a broad range of excitation, high photoluminescence quantum yield (PL QY), and strong photo and chemical stability. A variety of materials, including organic, inorganic, polymers, metal nanoparticles and quantum dots, has been proposed and



successfully tested to participate in efficient light harvesting studies. Among them, quantum dots stand out due to its unique size dependent photophysical properties. Quantum dots are semiconductor nanocrystals that exhibit size dependent quantum confinement of the electron-hole pair when its size is reduced to a regime lower than the Bohr excitonic radius (**Scheme 1.2**).<sup>9</sup> Quantum confinement is defined by the collapse of the continuum of energy levels (in bulk materials) to discrete, atomic like levels of energy accompanied with an increase in the energy band gap,  $E_g$ .



**Scheme 1.2:** A schematic showing the effect of quantum confinement on tuning the optical properties in a size dependent manner, from molecule to bulk. (Redrawn from ref. 9)

The interesting size tunable optoelectronic properties of QDs have been explored in broad areas of science and technology ranging from bio-imaging to light harvesting.<sup>10,11</sup> However, the pragmatic use of QDs are still limited as most of the studies have been carried out primarily on highly toxic metal ion based QDs such as CdTe, CdSe, PbS, PbSe, ZnSe etc.<sup>12,13</sup> This has diverted the attention of researchers in the search of environmentally friendly and less toxic metal ion based QDs. In this regard, InP/ZnS and CuInS<sub>2</sub>/ZnS based QDs have emerged as promising alternates in the recent years.<sup>14,15</sup> Appreciable knowledge has been gained over the last decade on the fundamental photophysical and light harvesting properties on such eco-friendly QDs in organic solvents.<sup>15</sup> However, similar knowledge is scarcely known in aqueous medium, which is

crucial to expand the scope of eco-friendly QDs to biomedical research. Thus, attempts have been made recently to address this challenge and have shown the successful use of InP/ZnS QDs as an efficient FRET donor in aqueous medium.<sup>16</sup> Many more such studies with different donor-acceptor systems (visible and NIR emitting dyes, biomolecules etc.) are still required to understand and optimize various light harvesting processes. In this regard, the present study focuses on ternary CuInS<sub>2</sub>/ZnS QDs and tests their ability to act as donors in light harvesting studies, in aqueous medium. Apart from being environmentally friendly, CuInS<sub>2</sub> QDs also exhibit a tunable PL emission from visible to NIR region which renders them all the more favorable for biological studies. The NIR emitting eco-friendly CuInS<sub>2</sub> QDs were successfully transferred from organic to aqueous medium using a place exchange protocol, with ~60% retainment of its photoluminescence quantum yield. All the photophysical studies confirm a highly efficient electrostatically driven photoinduced electron transfer process between oppositely charged CuInS<sub>2</sub> QD donor and Indocyanine green (ICG) acceptor molecules.

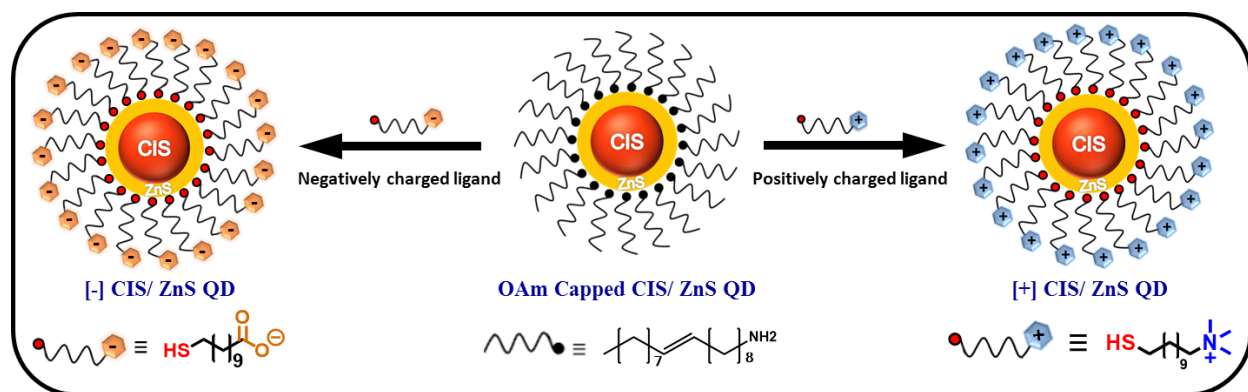
## 2. Experimental section:

**Chemicals:** Indium acetate (In(Ac)<sub>3</sub>), Copper acetate (Cu(Ac)<sub>2</sub>), 1- Dodecanethiol (DDT), 1-Octadecene (ODE), Oleic acid (OA), Zinc stearate (Zn(St)<sub>2</sub>), Oleylamine (OAm), Sodium (Na), Trimethylamine hydrochloride (TMAH), 11-Bromoundecene, Thioacetic acid (TA), Azobisisobutyronitrile (AIBN), Indocyanine green (ICG) and Methylene Blue (MB) were purchased from Sigma-Aldrich and were used without further purification. N,N,N-trimethyl(11-mercaptoundecyl)ammonium chloride (TMA) was synthesized using a reported procedure.<sup>17</sup>

**2.1. Synthesis of CIS QDs:** CuInS<sub>2</sub>/ZnS core-shell quantum dots were synthesized following a reported protocol.<sup>18</sup> Briefly, In(Ac)<sub>3</sub> (0.2mmol, ~58mg) and Cu(Ac)<sub>2</sub> (0.2mmol, ~36mg) were mixed with DDT (8.35mmol, 2mL), 0.3mL OA and 3mL ODE in a 50mL three-neck RB and gently stirred under N<sub>2</sub> atmosphere. The reaction mixture was heated at 100°C for 10 min until a clear solution was obtained. Subsequently, vacuum was applied for 30 min and the reaction temperature was raised to 230°C to allow the growth of CuInS<sub>2</sub> QDs for 15 min. With the increase in temperature, the reaction solution changed color from light yellow to yellow to red and finally dark red,

indicating nucleation and formation of  $\text{CuInS}_2$  QDs. The reaction was quenched by lowering the temperature to  $50^\circ\text{C}$  using a water bath. For in-situ ZnS overcoating, a solution of ODE and OAm (4:1 ratio, 1.6mL and 0.4 mL respectively) containing  $\text{Zn}(\text{St})_2$  (0.2mmol,  $\sim 125\text{mg}$ ) was added dropwise to the reaction mixture at  $160^\circ\text{C}$  under  $\text{N}_2$  flow over a period of 30 min. Subsequently, the reaction temperature was increased to  $230^\circ\text{C}$  and retained for 2 h to allow for shell growth. The reaction was quenched by lowering the temperature to  $50^\circ\text{C}$  and precipitating with ethanol. The precipitates were purified three times by centrifugation at 7500rpm for 10 min and redispersed in chloroform for further studies.

**2.2. Preparation of water soluble CIS QDs:** Water soluble cationic [+] CIS QDs were prepared via a place exchange reaction (**Scheme 2.1**). To a solution containing cationic TMA ligand (100mg) dissolved in 1:1 ratio of methanol: water, OAm capped CIS QDs in chloroform ( $1\mu\text{M}$ , 5mL) were added and stirred for  $\sim 4$  h. The progress of the phase transfer reaction can easily be monitored by observing the color changes in the lower organic (dark red to colorless) and upper aqueous (colorless to dark red) phases. The TMA ligand aided in stabilization of the QDs (through the thiol group) as well as in phase transfer (through the quaternary ammonium group) imparting cationic surface charge to the QDs. The aqueous layer was carefully removed and precipitated using isopropanol at 7500rpm for 10 min. Finally, the precipitates were redispersed in deionized water, yielding [+] CIS QDs. A similar procedure was adapted for preparing [-] charged CIS QDs by using a basic solution of [-] MUA ligand where the thiol group aided in surface functionalization and the carboxylic group assisted in imparting the [-] charge.



**Scheme 2.1:** Schematics representing the place exchange reaction between oleylamine amine (OAm) capped CIS QDs and [+] TMA / [-] MUA ligands, yielding water soluble [+] / [-] CIS QDs.

**2.3. Photoluminescence quenching experiments:** In a typical experiment, a 3mL aqueous solution of charged CIS QDs was prepared by optimizing the optical density at the excitation wavelength (450nm) to be ~0.1, corresponding to a concentration of ~0.6µM. With the QDs acting as donors, aliquots of acceptor dye molecules were sequentially added to the QD solution and the spectral changes were monitored, both in terms of absorbance and steady state photoluminescence quenching. Correspondingly, time resolved measurements via Time Correlated Single Photon Counting (TCSPC) system were carried out using 459nm laser as the excitation source. The fluorescence decay curves were fitted with tri-exponential functions with minimum  $\chi^2$  value. Similar procedure was adopted for the temperature dependent studies where the sample was allowed to equilibrate for 3 min at the set temperature before the measurement with a tolerance range of 0.5°C. In the same manner, polarity dependent studies were also carried out where the [+] CIS QDs were dispersed in a mixture of acetonitrile (ACN) and water of varying ratios. Experiments under inert conditions were also performed in a similar manner where the optical density of [+] CIS QDs were optimized to be ~0.1 at the excitation wavelength, following which 0.7µM of [-] ICG dye was added. The steady state and lifetime measurements were taken. After the measurements, the solution was purged with Ar for a period of 1h and the measurements were repeated.

**2.4. Stern-Volmer Analysis:** The nature of photoluminescence quenching between the donor and acceptor was analyzed using the Stern-Volmer equation<sup>19</sup>:

$$\frac{I_0}{I} = 1 + K_{SV}[Q]$$

where  $I_0$  and  $I$  are the donor fluorescence intensity in the absence and presence of the quencher, respectively.

[Q] is the quencher concentration (M).

$K_{SV}$  is the Stern-Volmer constant ( $M^{-1}$ ).

From the plot of  $I_0/I$  vs. the quencher concentration, with the intercept as 1,  $K_{SV}$  can be obtained from the slope. The Stern-Volmer constant,  $K_{SV}$ , is given as:

$$K_{SV} = k_q \cdot \tau_0$$

where  $k_q$  is the bimolecular quenching constant ( $M^{-1}s^{-1}$ ).

$\tau_0$  is the lifetime of the donor (ns).

### 3. Instrumentation and Techniques used:

**3.1. UV-Vis absorption studies:** The absorption studies were performed in Shimadzu UV-3600 Plus UV-Vis/NIR spectrophotometer in a quartz cuvette of path length 1cm. The absorption was monitored over an entire range of 300nm - 1000nm. The concentration of the CIS QDs<sup>20</sup> was determined by using the Beer-Lambert law:

$$A = \epsilon \cdot c \cdot L$$

where A is the optical density (absorbance) at absorption maxima.

$\epsilon$  is the molar extinction coefficient at a particular wavelength ( $M^{-1}cm^{-1}$ ).

c is the concentration of the solution (M).

L is the optical path length (cm).

**3.2. Photoluminescence studies:** The photoluminescence experiments were carried out in Fluorolog-3 spectrofluorometer (HORIBA Scientific) with Xe- lamp as the excitation source. The sample was excited at a wavelength of 450nm where the dye acceptor molecules (ICG and MB) had negligible absorption.

**3.3. Time resolved measurements:** Time resolved studies were performed by using Time Correlated Single Photon Counting (TCSPC) system. The experiments were carried out using a 459nm NanoLED as the excitation source with a time-to-amplitude converter (TAC) range of 1000ns for 10,000 counts. The decay curves were deconvoluted and fitted using DAS analysis software v.6.5.6.

**3.4. Zeta potential measurements:** Zeta potential ( $\zeta$ ) was used to characterize the surface charge on the CIS QDs. The measurements were carried out in Zetasizer Nano series, Nano-2590 (Malvern instruments, U.K.) having a 655nm laser. The zeta potential is measured in terms of the electrophoretic mobility ( $U_E$ ) (the velocity with which the charged particles are attracted to the oppositely charged electrodes) and is calculated using Henry's equation<sup>21</sup>:

$$U_E = \frac{2\varepsilon\zeta f(ka)}{3\eta}$$

where  $\varepsilon$  is the dielectric constant of the medium.

$\zeta$  is the zeta potential (mV).

$f(ka)$  is the Henry's function (value from Smoluchowski's approximation).

$\eta$  is the viscosity of the medium (Pa.s).

**3.5. X-Ray Diffraction (XRD) measurements:** Powder XRD was performed to confirm the crystal lattice structure of CIS QDs. The measurements were carried out in Bruker D8 Advanced X-Ray Diffractometer using Cu K $\alpha$  ( $\lambda = 1.54 \text{ \AA}$ ) rays. The lattice spacing ( $d$ ) in the crystalline sample was estimated using Bragg's law:

$$n\lambda = 2d \sin \theta$$

where  $n$  is the order of diffraction.

$\lambda$  is the wavelength of incident X-rays (nm).

$\theta$  is the scattering angle.

By scanning the sample through a range of  $2\theta$  angles, all the possible diffraction angles can be obtained which can be used to confirm the crystal structure of the sample.

**3.6. High Resolution Transmission Electron Microscopy (HRTEM):** The sample was prepared by drop casting 10 $\mu$ L of CIS QDs solution on a 400-mesh carbon coated copper TEM grid (Ted Pella, Inc.). The sample was allowed to dry under ambient conditions and was further dried under vacuum. The image was taken in TECNAI G2 20 TWIN at 200keV.

## 4. Results and Discussion:

**4.1. Characterization of CIS QDs:** The positively ([+]) and negatively ([−]) charged CIS QDs were prepared through a place exchange reaction, and well characterized using various spectroscopic and microscopic techniques (**Figure 4.1**). The steady state photophysical measurements showed negligible changes in the absorption and PL maxima of the CIS QDs upon place exchange reaction. The first excitonic peak and PL maxima of CIS QDs were observed  $\sim$ 534nm and  $\sim$ 680nm respectively, with a full width at half maxima (*fwhm*) of  $\sim$ 75 nm. The broad emission spectra with a high *fwhm* value is attributed to the absence of near-band edge emission in case of QDs such as CIS

owing to the higher proportion of surface defects such as Cu and In vacancies and interstitials. As a result, the emission observed is generally from the surface related trap states.<sup>22,23</sup> Interestingly, ~60% of the PL QY was retained after the place exchange reaction with both, [+] TMA and [-] MUA, ligands.

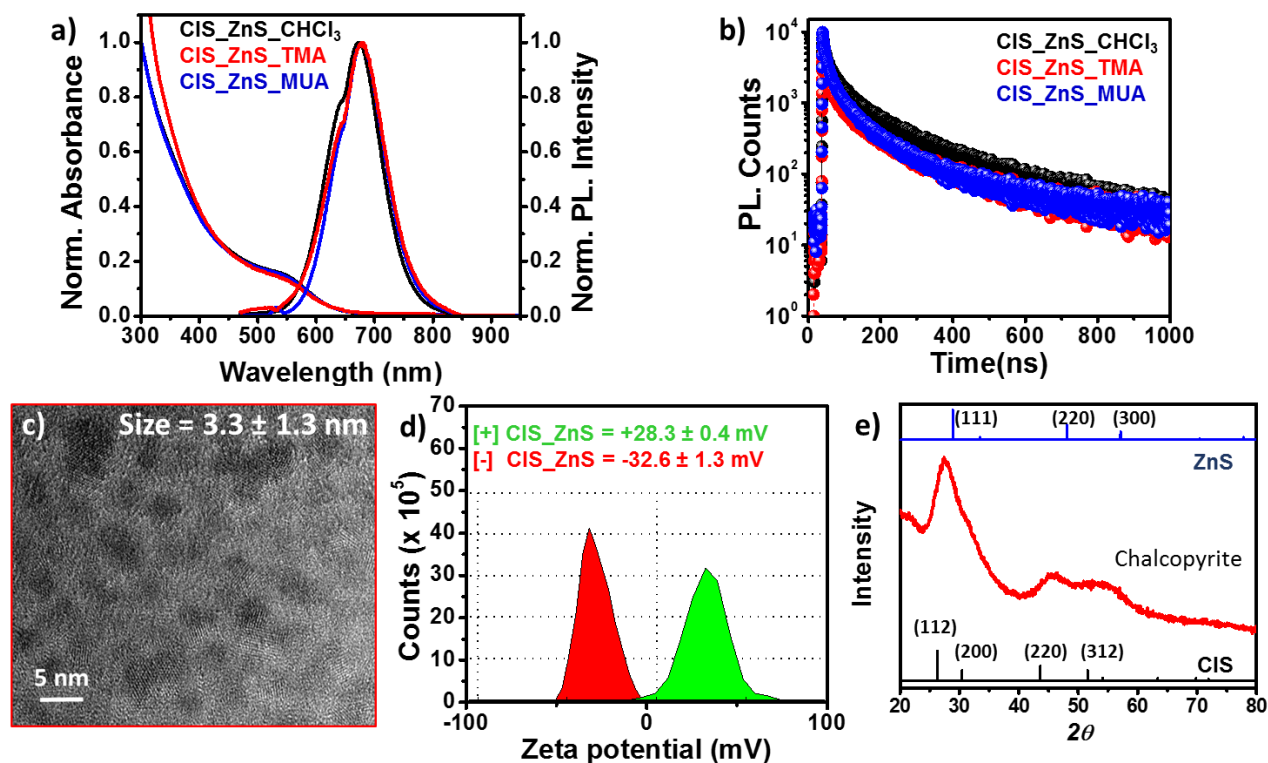


**Figure 4.1: Spectroscopic and microscopic characterization of water soluble CIS QDs.** (a) The normalized absorption and PL spectra of CIS QDs before and after water solubilization. (b) The PL decay profiles of CIS QDs before and after place exchange reaction. (c) A representative HRTEM of [+] CIS QDs. (d) Zeta potential of [+] and [-] CIS QDs. (e) XRD data of CIS QDs.

The tri-exponential PL decay profile was retained in [+] and [-] CIS QDs as well, with an average lifetime value of ~120 ns and ~ 100 ns, respectively. The core diameter of CIS QDs was estimated to be 3.3 ± 1.3nm from HRTEM studies. XRD data confirmed the chalcopyrite structure of the CIS QDs, which is in agreement with the literature reports.<sup>24</sup> The surface charges on CIS QDs were characterized by zeta potential measurements, which showed a zeta potential of +28.3 ± 0.4 mV and -32.6 ± 1.3 mV for [+] and [-] CIS QDs, respectively.

**4.2. Photoluminescence quenching studies:** The photoluminescence quenching studies were undertaken with the motivation of developing efficient light harvesting systems based on CIS QDs in the NIR region, in aqueous medium. The NIR emitting Indocyanine green (ICG) was selected as the acceptor molecule. ICG dye exhibit the absorption and emission maxima  $\sim 779\text{nm}$  and  $803\text{nm}$  in aqueous solvent, respectively (**Figure 4.2**). Also, ICG possess a net negative charge which can participate in strong electrostatic attraction with  $[+]$  CIS QDs.

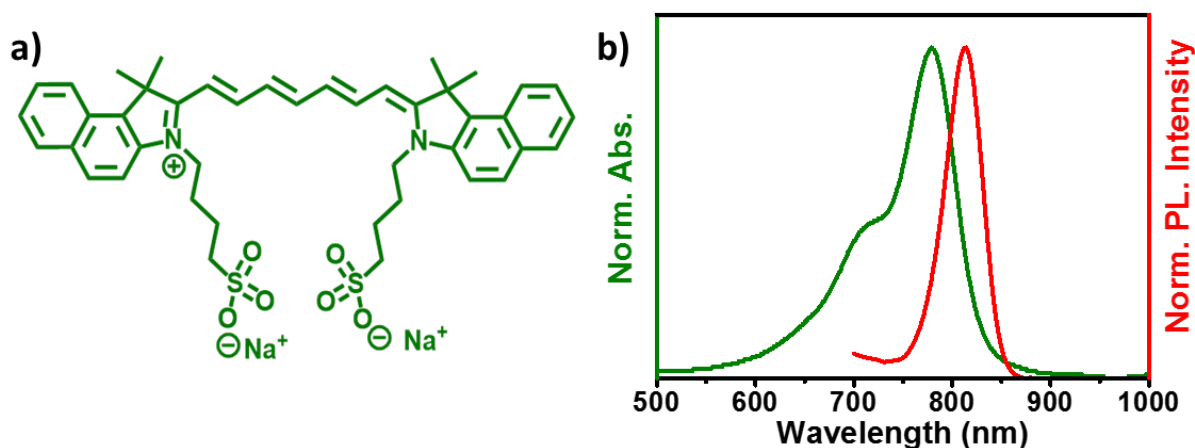
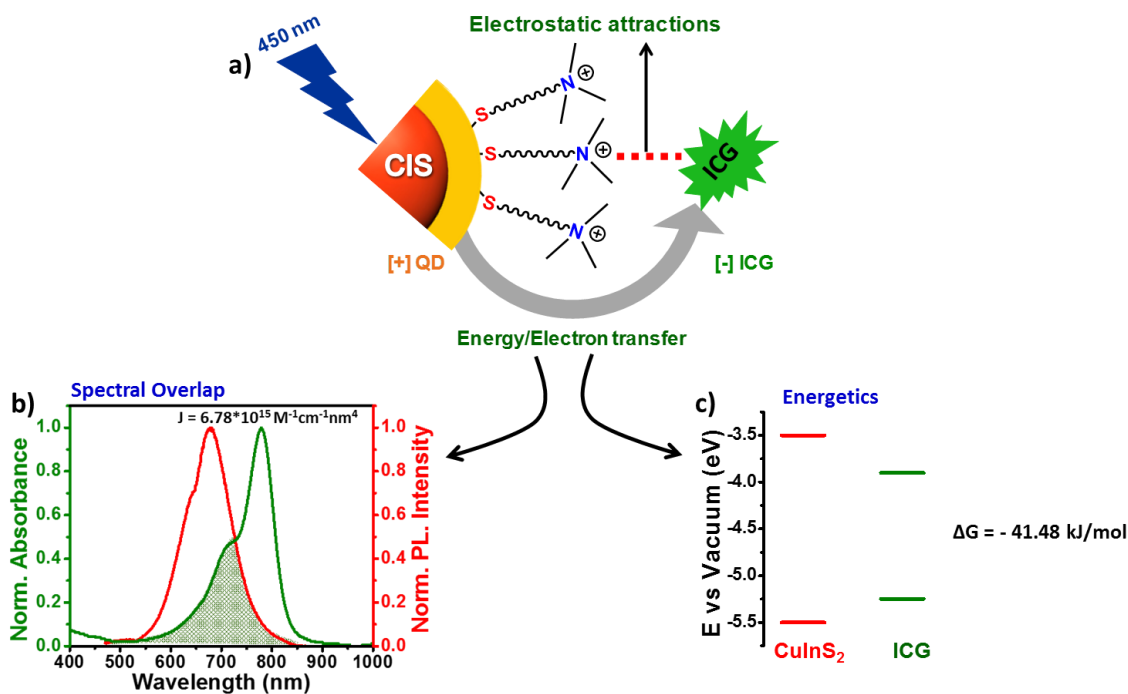


**Figure 4.2: Characteristics of ICG dye molecule. (a)** Chemical structure of ICG dye. **(b)** The absorption and emission spectra of ICG dye in water.

An in-depth analysis on the photophysics and energetics of CIS QDs and ICG dye revealed the following points. The spectral overlap integral ( $J$ ) between the PL of CIS QDs and the absorption of ICG dye was estimated to be  $\sim 6.78 \times 10^{15} \text{ M}^{-1}\text{cm}^{-1}\text{nm}^4$ , indicating that CIS and ICG forms an effective FRET donor-acceptor pair (**Figure 4.3a**). At the same time, the calculation of energy values (from absorption and cyclic voltammetry measurements) showed that an electron transfer from the photoexcited CIS QDs to ICG dye is thermodynamically feasible ( $\Delta G = -41.5 \text{ kJ/mol}$ ) (**Figure 4.3b**). Hence, it can be concluded that the CIS QD - ICG pair can, in principle, participate in both energy and electron transfer processes. Accordingly, detailed photophysical studies based on both steady state and time resolved spectroscopy were carried out to understand the mode of interaction between the  $[+]$  CIS QDs and  $[-]$  ICG dye molecules.





4

**Figure 4.3: Conditions for plausible energy and electron transfer processes.** (a) A schematic representation of the plausible PL quenching process occurring between [+] CIS QDs and [-] ICG dye. (b) Spectral overlap between the PL of [+] CIS QDs and the absorption of [-] ICG dye. (c) Energy levels of [+] CIS QDs and [-] ICG dye.

Systematic photoluminescence quenching studies were performed by titrating small aliquots (3  $\mu\text{L}$  of 0.14 mM) of [-] ICG dye molecules to  $\sim 0.6 \mu\text{M}$  [+] CIS QDs (**Figure 4.4**). A bathochromic shift of  $\sim 27 \text{ nm}$  was observed in the absorption of [-] ICG dye molecules in the presence of [+] CIS QDs, indicating the possibility of a strong ground state interaction. A steady and gradual decrease in the PL of [+] CIS QDs was observed upon the addition of ICG molecules, without the emergence of any PL corresponding to ICG. This rule out the possibility of FRET as the main mechanism for the quenching the PL of CIS QDs. The ground state interaction was further confirmed through Stern-Volmer analysis. The Stern-Volmer ( $K_{\text{SV}}$ ) and the bimolecular quenching ( $k_{\text{q}}$ ) constants were determined from the  $I_0/I$  vs quencher concentration plot (**Figure 4.4c**). The high  $k_{\text{q}}$  value of  $\sim 4 \times 10^{13} \text{ M}^{-1} \text{ s}^{-1}$  (greater than the diffusion controlled  $k_{\text{q}}$ ;  $\sim 1 \times 10^{10} \text{ M}^{-1} \text{ s}^{-1}$ ) confirms a strong ground state interaction between the [+] CIS QD donor and [-] ICG acceptor molecules. The steady state quenching efficiency<sup>16</sup>,  $E$ , was calculated to be  $\sim 85\%$  using the formula:

$$E = 1 - \frac{I}{I_0}$$

where,  $I$  and  $I_0$  are the PL intensity of the donor in the presence and absence of the acceptor.

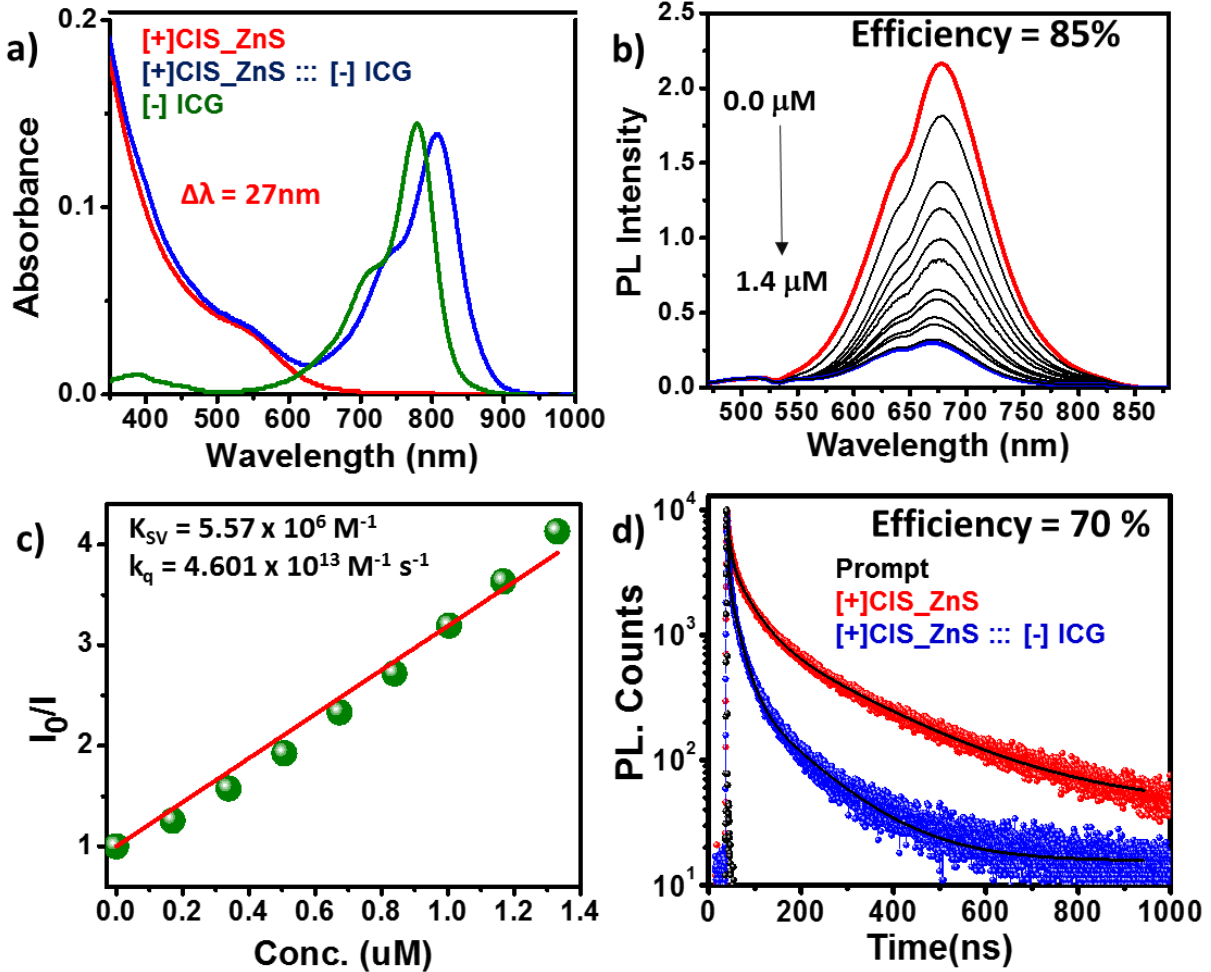


**Figure 4.4: Photoluminescence quenching studies in [+ ] CIS QD – [- ] ICG dye nano hybrid.** (a) The absorption spectra of [- ] ICG dye in absence and presence of [+ ] CIS QDs. (b) Spectral changes in the PL of [+ ] CIS QDs upon sequential addition of [- ] ICG dye. (c) Stern-Volmer plot corresponding to PL quenching of [+ ] CIS QDs by [- ] ICG dye. (d) PL decay profile of [+ ] CIS QDs in the absence and presence of [- ] ICG dye, collected at the QD emission of 680 nm.

The quenching of CIS QD PL was confirmed using Time-Correlated Single Photo Counting (TCSPC) studies. A clear quenching in the PL decay of [+ ] CIS QDs was observed in the presence of [- ] ICG dyes. The lifetime of [+ ] CIS QDs was estimated to be  $\sim 36$  ns in the presence of  $\sim 1.4 \mu\text{M}$  of [- ] ICG dye. An efficiency<sup>16</sup> of  $\sim 70\%$  was estimated from time resolved PL quenching studies using the following formula:

$$E = 1 - \frac{\tau}{\tau_0}$$

where,  $\tau$  and  $\tau_0$  are the lifetime of the donor in the presence and absence of the acceptor. This is in good agreement with the steady state quenching studies.

Now, there can be two main mechanisms for the quenching of [+] CIS QD PL by [-] ICG molecules: namely FRET and electron transfer. The absence of ICG acceptor peak in the steady state and time-resolved PL studies rules out the possibility of FRET as the main mechanism for the quenching of CIS QDs. Thus, the role of electron transfer as the main quenching mechanism was investigated further.

**4.3. Proof for photoinduced electron transfer (PET):** In an electron transfer process an electron is transferred from the photoexcited state of donor to the acceptor, resulting in the formation of transient radical cation and radical anion respectively. The oxygen content, solvent polarity and temperature are well known to affect the efficiency of all the electron transfer processes. Accordingly, the PL quenching of [+] CIS QDs by [-] ICG molecules was studied by varying the above-mentioned parameters.

**4.3.1. Comparison of photoluminescence quenching studies in ambient and inert conditions:** Molecular oxygen is a well-known fluorescence quencher for almost all the known fluorophores.<sup>25</sup> The quenching of fluorescence by the paramagnetic oxygen is by directing the photoexcited fluorophore to undergo an intersystem crossing from a singlet to a triplet state.<sup>19</sup> Moreover, molecular oxygen is a highly reactive diatomic gas that can act as an efficient electron acceptor. Thus, molecular oxygen can act as an 'electron scavenger'<sup>26</sup> in the present study as well. Hence, comparing the PL quenching efficiencies under ambient and oxygen free (inert) conditions can serve as a direct evidence for electron transfer process between [+] CIS QD and [-] ICG.

Photoluminescence quenching studies were performed under ambient and inert (Ar purging) conditions with  $\sim 0.6 \mu\text{M}$  [+] CIS QD solution containing  $0.7 \mu\text{M}$  of [-] ICG dye (**Figure 4.5**). A steady state quenching efficiency of 25% was obtained in ambient condition, which increased to 45% upon Ar purging (**Table 4.1**). Complementing the trend observed in steady state, lifetime efficiencies also showed an increase in the quenching efficiency from 23% in ambient condition to 42% with Ar purging. The increase in the quenching efficiencies, under inert condition, can be attributed to the

absence of an additional quencher (O<sub>2</sub>), thereby favoring a more efficient photoinduced electron transfer from [+] CIS QD donor to [-] ICG dye acceptor molecules.

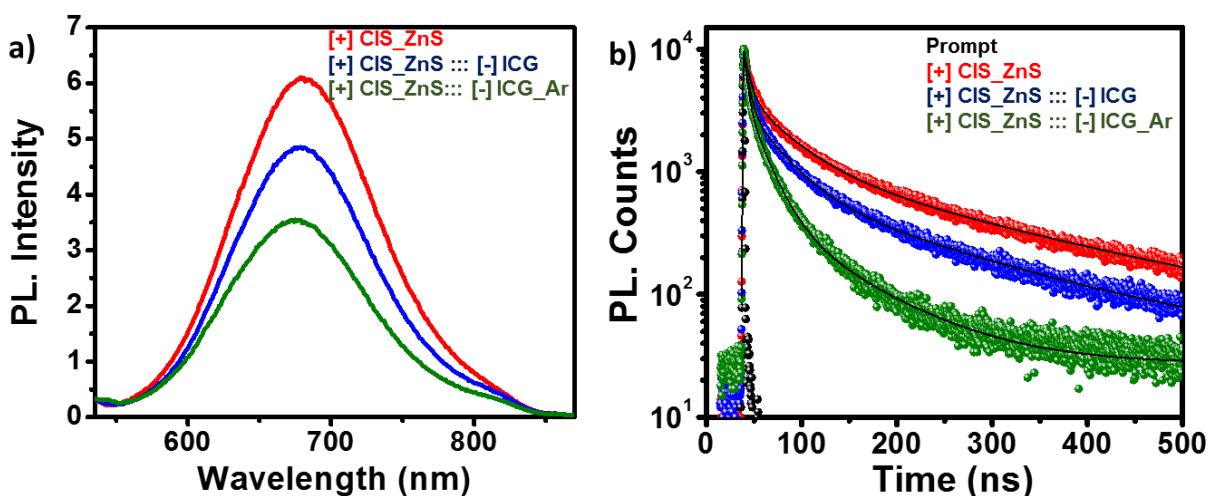


**Figure 4.5:** PL quenching studies in ambient and inert conditions. (a) Steady state and (b) Time resolved PL quenching of [+] CIS QDs by [-] ICG dye, before and after purging with Argon.

**Table 4.1:** Comparison of steady state and PL decay quenching efficiencies of [+] CIS QDs by [-] ICG dye before and after purging with Ar.

[+] CIS QD :: [-] ICG	Before Ar purging	After Ar purging
PL. quenching Efficiency (Steady State)	25%	45%
PL. quenching Efficiency (Lifetime)	23%	42%

**4.3.2. Effect of solvent polarity on photoluminescence quenching studies:** The effect of solvent polarity on the rate of electron transfer can be understood in terms of solvent reorganization energy. The solvent molecules play an important role in stabilizing the radical cation and radical anion formed during the electron transfer process. The charge transfer complex formed as a result of the excited state electron transfer process is more stabilized in a polar medium compared to a non-polar solvent, resulting in a higher efficiency of electron transfer in polar solvents.<sup>27</sup> The reorganization energy associated with polar solvents is higher than that of a non-polar

solvent.<sup>28</sup> In a non-polar medium, the free energy associated with the radical ion pair state is higher than that of the locally excited state, and the charge transfer reaction becomes thermodynamically unfavorable.<sup>28</sup> This can be explained on the basis of Rehm-Weller equation where the change in free energy for the formation of the charge transfer complex is higher in a polar medium due to the higher dielectric constant.<sup>19</sup> Hence, the effect of varying the solvent polarity can be used as a validation for the PET process occurring in the present system.

Accordingly, systematic PL quenching studies were performed in aqueous solution (dielectric constant,  $\epsilon = 78.36$  at 293K)<sup>29</sup> as well as in a mixture of 1:1 ratio of ACN: water (dielectric constant,  $\epsilon = 53.17$  at 293K)<sup>29</sup>. In both the solvent media, a gradual decrease in the steady-state PL intensity of [+] CIS QDs was observed upon addition of [-] ICG molecules. The PL quenching in both the solvent media is summarized in terms of Stern-Volmer plot (**Figure 4.6**). A higher quenching efficiency of ~80% was observed in aqueous solution as compared to that of ~65% in ACN: water mixture (**Table 4.2**). A similar trend was also observed in the lifetime quenching efficiencies, with an efficiency of ~70% in aqueous solution and ~60% in ACN: water mixture.

The above results confirm the occurrence of a more efficient quenching process in a more polar system. As mentioned earlier, PET is highly dependent on the solvent polarity and is more favored in a polar system. Hence, it is possible to further ascertain that the mode of interaction between [+] CIS QD donor and [-] ICG dye acceptor is PET.

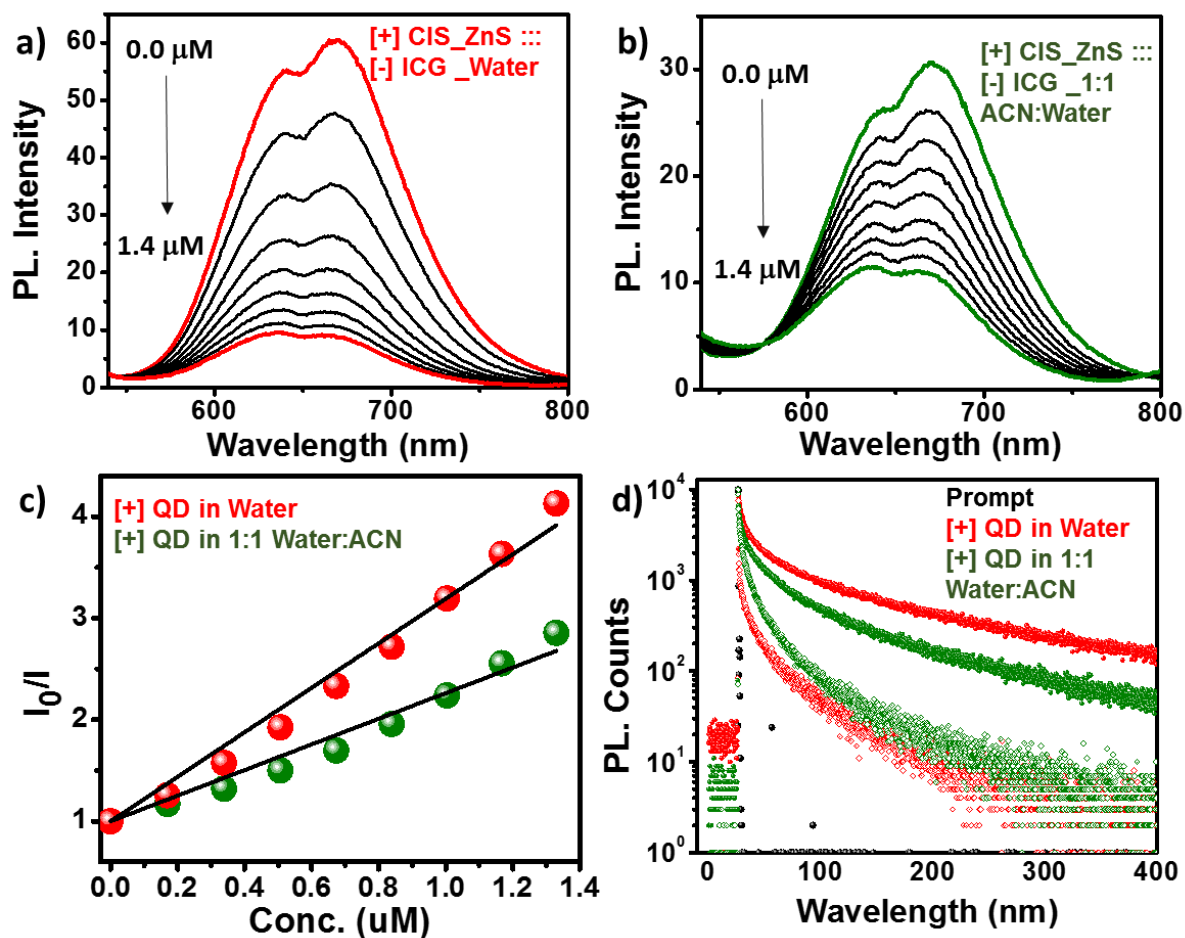


**Figure 4.6: Effect of solvent polarity on PL quenching.** Steady state PL spectral changes of [+] CIS QDs upon the addition of [-] ICG dye in (a) water and (b) 1:1 water:ACN solvent mixture. The corresponding Stern-Volmer plots are showed in (c). (d) PL decay profile of [+] CIS QDs in the presence and absence of [-] ICG dye, as a function of solvent polarity.

**Table 4.2: Comparison of steady state and PL decay quenching efficiencies of [+] CIS QDs by [-] ICG dye as function of solvent polarity.**

Sample	PL. quenching Efficiency (steady state)	PL. quenching Efficiency (lifetime)
QD – Water ( $\epsilon = 78.36$ )	80%	70%
QD – 1:1- Water:ACN ( $\epsilon = 53.17$ )	65%	60%

**4.3.3. Effect of temperature on photoluminescence quenching studies:** The efficiency of electron transfer depends on temperature and Gibb's free energy change of the process.<sup>30</sup> The temperature dependence of PET can be explained in terms of the activation energy. A rise in temperature increases helps in crossing the activation barrier, thereby increasing the rate of electron transfer.<sup>31</sup> Accordingly, the effect on temperature on the PL quenching of [+] CIS QDs by [-] ICG was investigated.

The steady state PL quenching studies were performed at three different temperatures: 283K, 298K, and 308K (**Figure 4.7.1**).

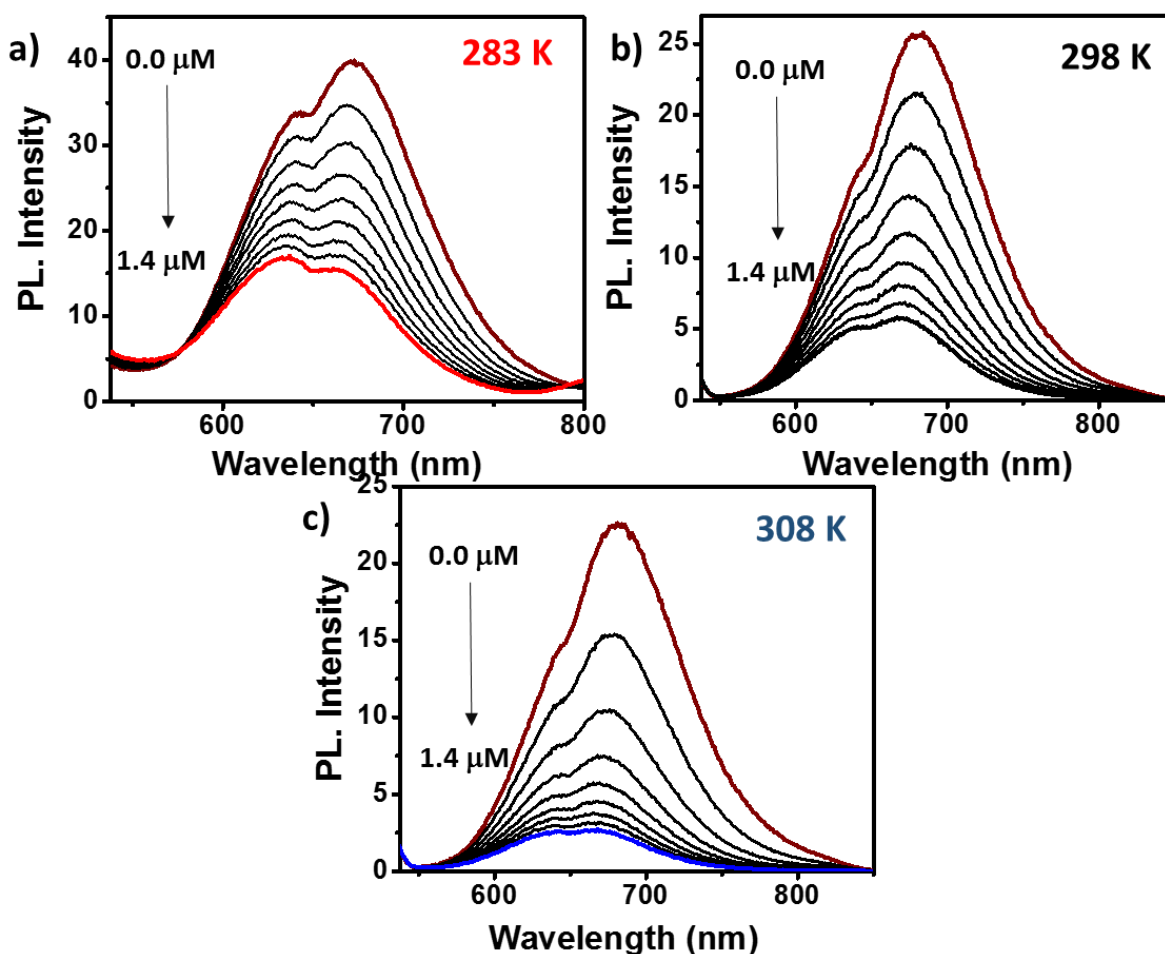


**Figure 4.7.1: Effect of temperature on PL quenching.** The steady state PL quenching of [+] CIS QDs by [-] ICG dye molecules in different temperatures are shown in (a) 283 K. (b) 298 K. (c) 308 K.

The PL quenching at different temperatures is summarized in terms of Stern-Volmer plot (**Figure 4.7.2**). It was observed that the slope of the Stern-Volmer plot increased

as the temperature increased, confirming an increase in the quenching efficiencies. All the above PL quenching studies confirm that the PL quenching in [+] CIS QD by [-] ICG is predominantly through a photoinduced electron mechanism.

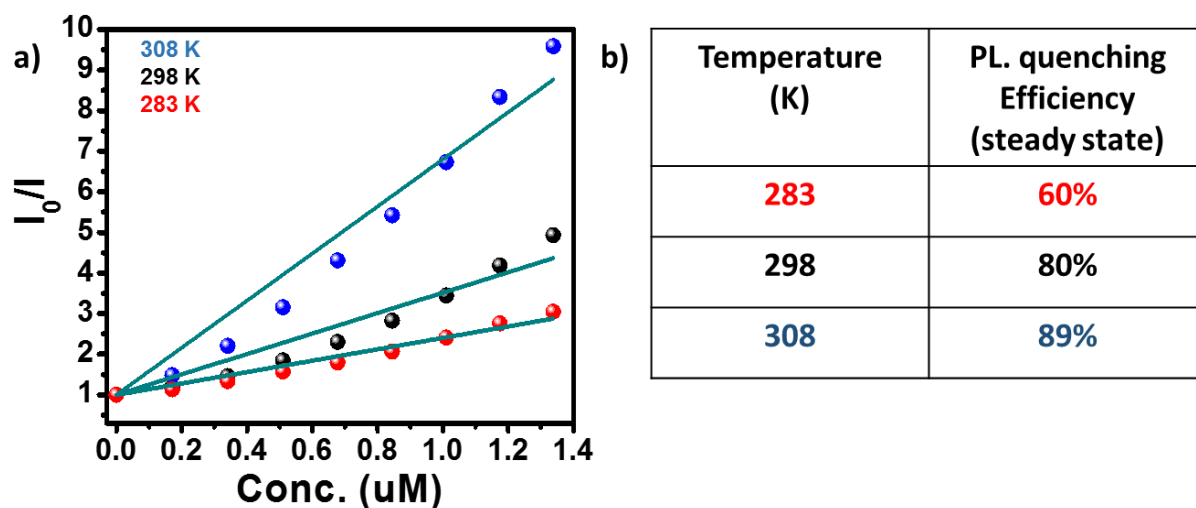


**Figure 4.7.2: Effect of temperature on PL quenching.** (a) Stern-Volmer plot and (b) table showing the PL quenching of [+] CIS QD by [-] ICG dye at different temperatures.

**4.4. Mode of interaction between CIS QD donor and ICG acceptor molecules.** The (i) large bathochromic shift in the absorption of ICG dye in the presence of CIS QDs and (ii) high bimolecular quenching constant indicate a strong binding interaction between CIS and ICG. The presence of [+] and [-] charges on CIS QDs and ICG molecules point to the possibility of electrostatic attraction as the main mode of interaction for the formation of a strong ground state complex. The following control experiments were performed to ascertain the role of electrostatics in the efficient electron transfer process between [+] CIS QDs and [-] ICG molecules.

**4.4.1. Reduction in electrostatic attraction:** One of the strategies which were adopted to portray the significance of electrostatic interaction was the introduction of electrostatic repulsion to the system under study. This was achieved by using [-] CIS QDs instead of [+] CIS QDs as the donor moiety. Photoluminescence quenching studies were carried out by titrating small aliquots of [-] ICG dye to an aqueous solution of [-] CIS QDs. The PL quenching was monitored using both steady state and time



resolved techniques (Figure 4.8).

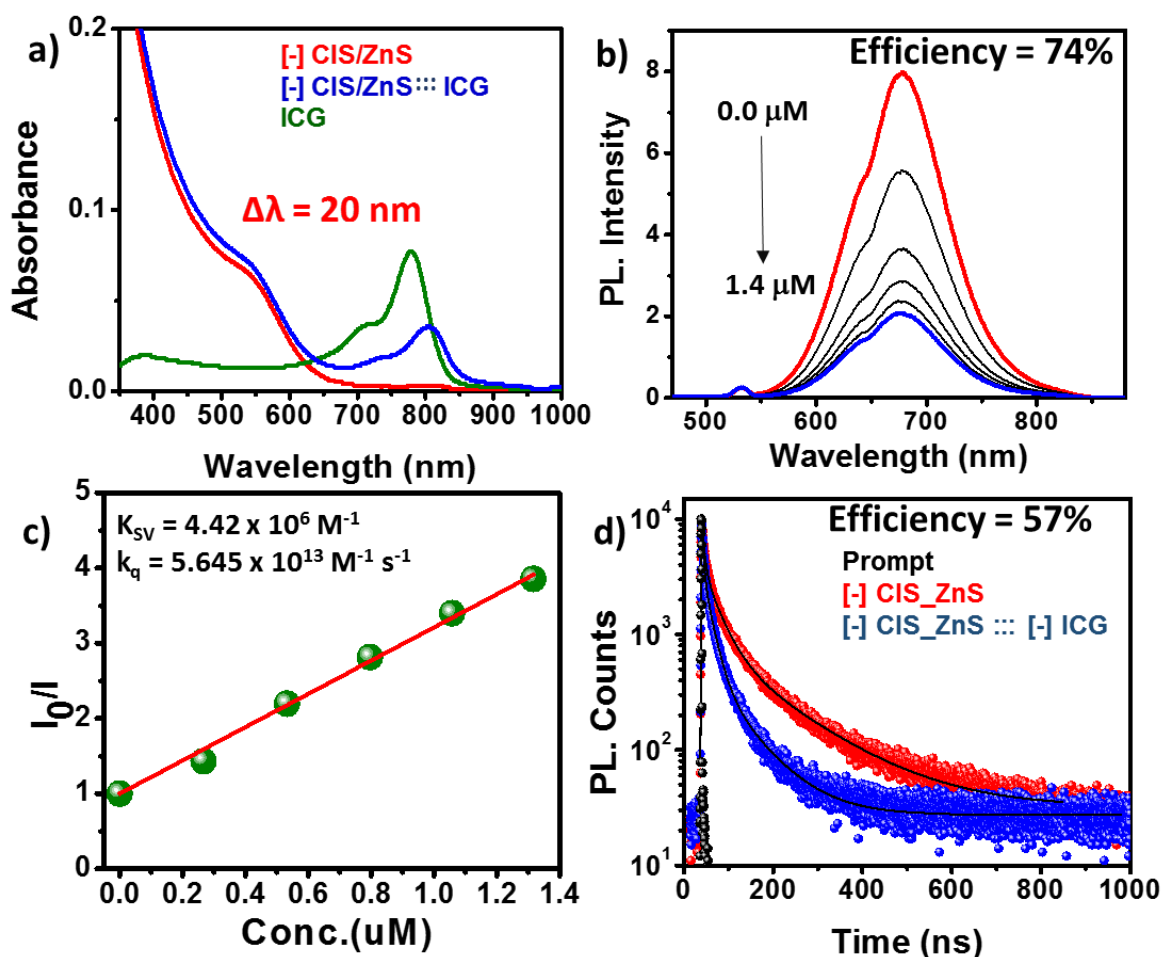
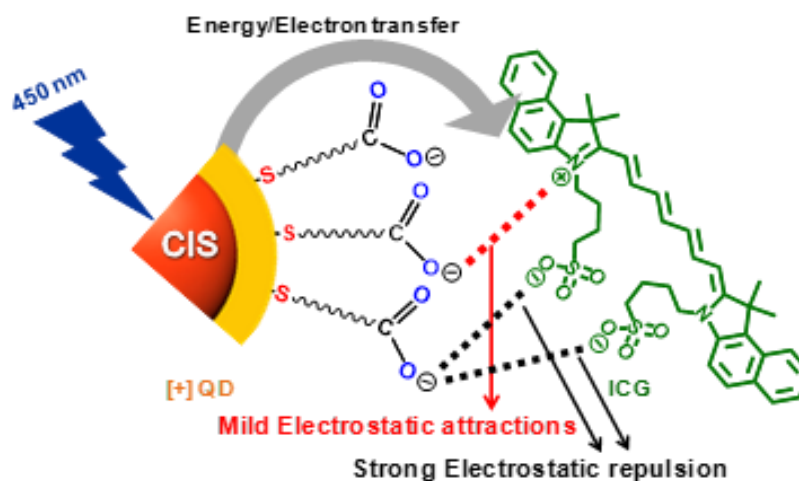


**Figure 4.8: PET between [-] CIS QDs and [-] ICG dye.** (a) Absorption spectra of ICG dye in the absence and presence of [-] CIS QDs. (b) Spectral changes in steady state PL emission of [-] CIS QDs upon addition of varying concentrations of [-] ICG dye, and (c) the corresponding Stern-Volmer plot. (d) PL decay profile of [-] CIS QDs in the absence and presence of [-] ICG dye.

A lower bathochromic shift of  $\sim 20$  nm was observed in the absorption spectra of [-] ICG dye in the presence of [-] CIS QDs, as compared to a shift of  $\sim 27$  nm in the presence of [+] CIS QDs. A careful examination of the structure of ICG molecule reveals that it has two [-] charges (via sulphonate groups) and one [+] charge (via quarternary amine group). This can lead to the complexation between [-] CIS QD and [-] ICG dye through the weak electrostatic attraction (**Scheme 4.1**). The PL quenching efficiencies between [-] CIS QD and [-] ICG molecules was estimated to be  $\sim 75\%$  and  $\sim 60\%$  using steady state and lifetime studies, respectively. There is an appreciable

decrease in the quenching efficiency compared to [+] CIS - [-] ICG donor-acceptor system. This confirms a comparatively weaker electrostatic attraction between [-] CIS QDs and [-] ICG molecules.



**Scheme 4.1:** A schematic representation of the electrostatic attraction and repulsions possible between [-] CIS QD donor and [-] ICG acceptor dye.

**4.4.2. Photoinduced electron transfer studies in organic solvent:** To further confirm and understand the significance of electrostatics, PL quenching studies were carried out with oleylamine (OAm) capped CIS QDs and ICG dye in chloroform ( $\text{CHCl}_3$ ) solvent (**Figure 4.9**). The absence of a bathochromic shift in the absorption spectra of ICG dye in the presence of CIS QDs in  $\text{CHCl}_3$ , indicates the absence of any strong ground state interaction between the CIS QDs and ICG dye molecules. Furthermore, the PL quenching efficiency of CIS QDs by ICG dye was less in  $\text{CHCl}_3$  as compared to water. For instance, a steady state efficiency of  $\sim 75\%$  was estimated in  $\text{CHCl}_3$  as compared to that of  $\sim 85\%$  in water. The PL quenching efficiency estimated from the lifetime studies corroborate the steady state results ( $\Phi_{\text{eff}(\text{CHCl}_3)} = 20\%$  vs  $\Phi_{\text{eff}(\text{H}_2\text{O})} = 70\%$ ). The large disparity between the two PL quenching efficiencies, in  $\text{CHCl}_3$ , estimated from steady state and lifetime studies confirm the role of non-radiative pathways in the PL quenching of CIS QD. A detailed analysis of the Stern-Volmer plot also shows a non-linear curvature towards the y-axis, confirming the involvement of both static and dynamic process in the quenching mechanism. Thus,

the decrease in the quenching efficiencies and absence of complex formation can be correlated to the lack of any specific interaction (such as electrostatic) between CIS QD donor and acceptor ICG dye in  $\text{CHCl}_3$ .

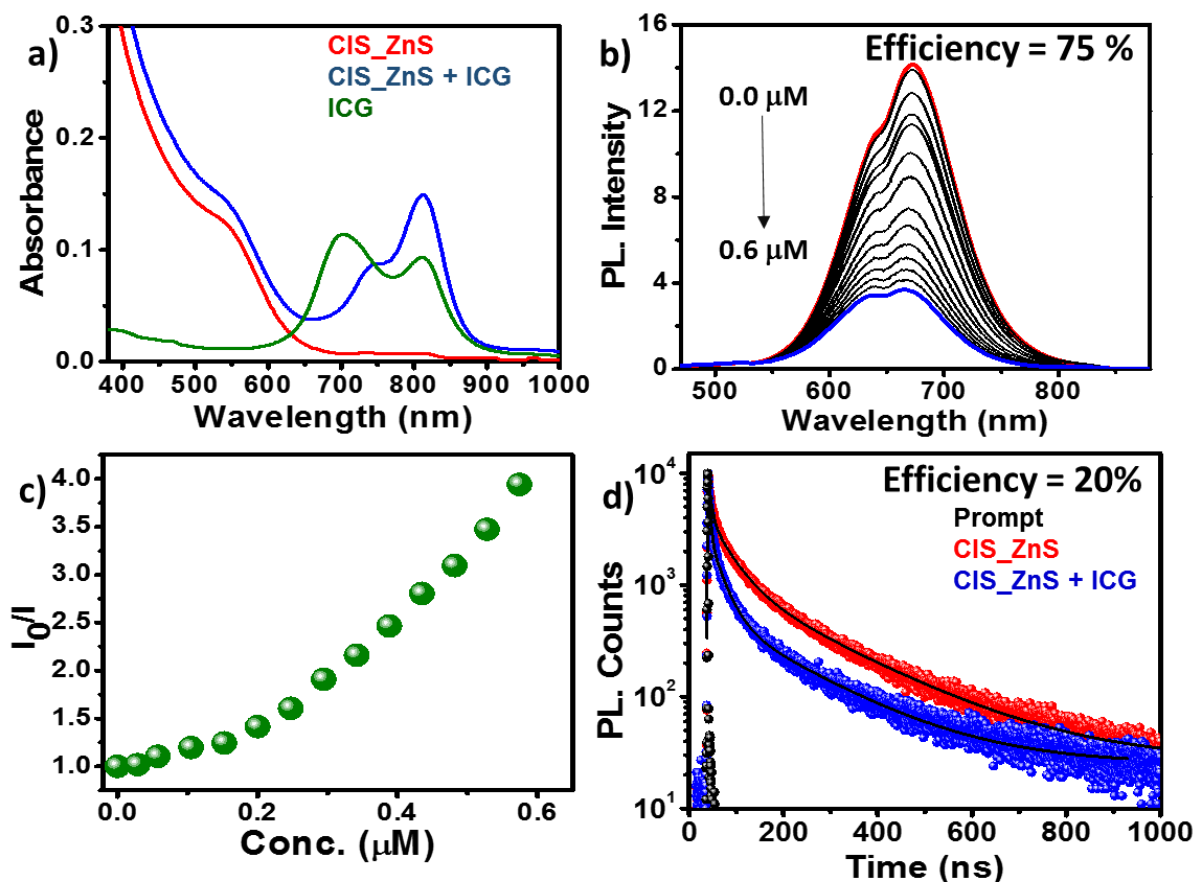


**Figure 4.9: PET in CIS QD – ICG dye nano hybrid in  $\text{CHCl}_3$ .** (a) Absorption spectra of ICG dye in the absence and presence of OAm capped CIS QDs. (b) Spectral changes in steady state PL emission of OAm capped CIS QDs upon addition of ICG dye, and (c) the corresponding Stern-Volmer plot. (d) PL decay profile of OAm capped CIS QDs in the absence and presence of ICG dye.

**4.5. Photoinduced electron transfer between [-] CIS QD and [+] Methylene blue dye:** In order to demonstrate the generality of our study as well as the exclusivity of electrostatic effect, PET studies were performed between [-] CIS QDs as donor and singly [+] charged methylene blue (MB) as the acceptor. MB dye has an absorption maximum  $\sim 665\text{nm}$  and an emission maximum  $\sim 683\text{nm}$  in aqueous medium (**Figure 4.10**).

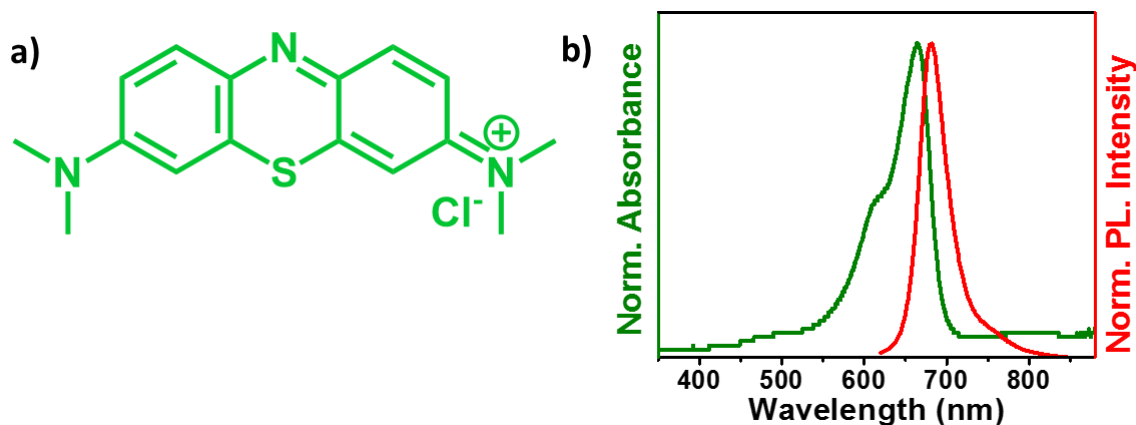


**Figure 4.10: Characteristics of methylene blue (MB) dye.** (a) Chemical structure of MB dye. (b) The absorption and emission spectra of MB dye in water.

A detailed analysis of the fundamental photophysics and energetics of [-] CIS QDs and [+] MB dye revealed that the pair forms efficient candidates for both FRET as well as PET (Figure 4.11).

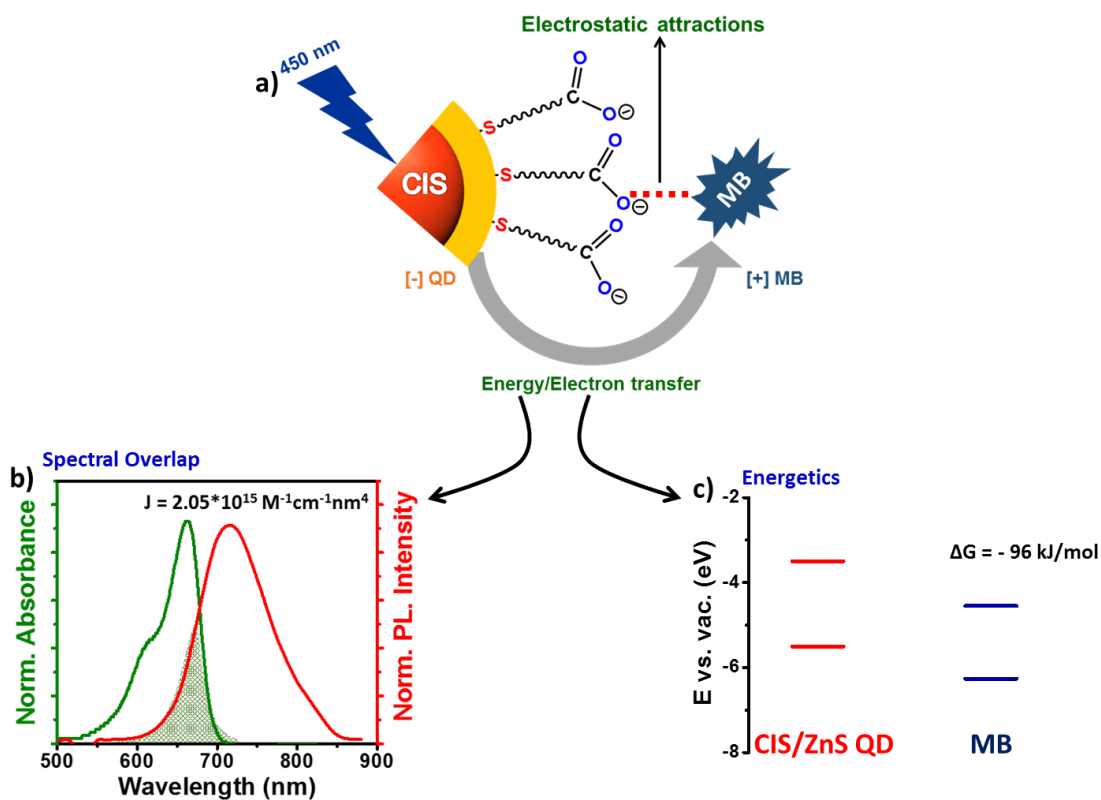


**Figure 4.11: Conditions for plausible energy and electron transfer processes in [-] CIS QD – [+] MB dye nanohybrid.** (a) A schematic representation of the plausible PL quenching

process occurring between [-] CIS QDs and [+] MB dye. **(b)** Spectral overlap between the PL of [-] CIS QDs and the absorption of [+] MB dye. **(c)** Energy levels of [-] CIS QDs and [+] MB dye.

The high spectral overlap integral (J) value of  $\sim 2 \times 10^{15} \text{M}^{-1} \text{cm}^{-1} \text{nm}^4$  indicates that the [-] CIS QD – [+] MB dye can form an efficient FRET donor-acceptor pair. At the same time, the energy levels also showed that an electron transfer from the photoexcited state of [-] CIS QDs to [+] MB is thermodynamically feasible ( $\Delta G = -96 \text{ kJ/mol}$ ).<sup>32</sup> Accordingly, detailed PL quenching studies using steady state and time resolved techniques were carried out.

**4.5.1. Photoluminescence quenching studies:** The PL quenching studies were performed by the sequential addition of small amounts of [+] MB dye molecules (3  $\mu\text{L}$  of 0.16 mM) to an aqueous solution of [-] CIS QDs ( $\sim 0.6 \mu\text{M}$ ). The spectral changes were monitored in terms of absorption, emission and lifetime measurements (**Figure 4.12**). In the presence of [-] CIS QDs, the absorption spectra of [+] MB showed a bathochromic shift of  $\sim 15 \text{nm}$  indicative of a strong ground state interaction. A gradual decrease in the emission of [-] CIS QDs was observed on subsequent addition of [+] MB dye, without the formation of any PL peaks corresponding to MB dye. The quenching efficiency was estimated to be  $\sim 90\%$  from steady state PL quenching studies. The Stern-Volmer analysis resulted in high  $k_q$  values ( $\sim 4 \times 10^{13} \text{M}^{-1} \text{cm}^{-1} \text{nm}^4$ ) confirming a strong ground state interaction between the [-] CIS QD donor and [+] MB acceptor molecules. The time resolved measurements also showed a PL quenching with an efficiency of  $\sim 65\%$ . The absence of any PL peak corresponding to MB in the steady state studies rules out the possibility of FRET between [-] CIS QDs and [+] MB dye. The most probable mechanism for the PL quenching of CIS QDs in the presence of MB molecules can be photoinduced electron transfer, as in the case of [+] CIS QD – [-] ICG nanohybrid.

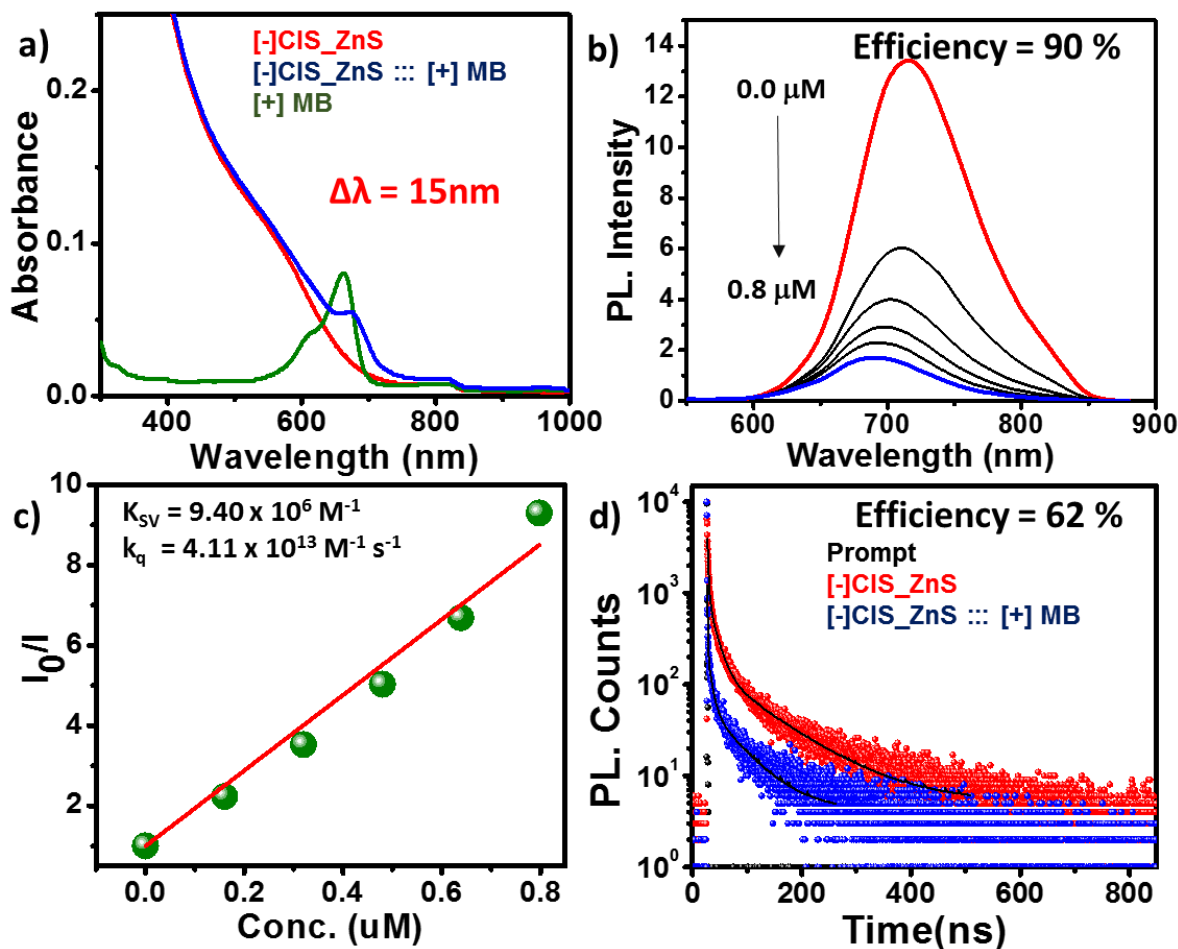


**Figure 4.12: Photoluminescence quenching studies in [-] CIS QD - [+] MB dye nanohybrid. (a)** The absorption spectra of [+] MB dye in the absence and presence of [-] CIS QDs. **(b)** Spectral changes in the PL emission of [-] CIS QDs upon sequential addition of [+] MB dye, and **(c)** the corresponding Stern-Volmer plot. **(d)** PL decay profile of [-] CIS QDs in the absence and presence of [+] MB dye, collected at the donor emission of 680nm.

**4.5.2. Demonstrating the role of electrostatics in CIS QD - MB nanohybrid:** The previous nanohybrid system of [+] CIS QDs and [-] ICG dye had both electrostatic attractive and repulsive interactions, which makes it difficult to prove the exclusivity of electrostatics in PET. On the other hand, [+] MB acceptor molecules can be an ideal system to prove the role of electrostatics in PET in CIS QDs. An efficient PET was observed between [-] CIS QD and [+] MB dye, as summarized previously. However, the use of [+] CIS QDs as donors failed to exhibit a noticeable PET with [+] MB under similar conditions (**Figure 4.13**). Unlike the previous case, the absorption spectra of [+] MB showed negligible changes in the presence of [+] CIS QDs suggesting the absence of any ground state interaction. Similarly, the steady state PL and lifetime

measurements also showed negligible changes in the PL of [+] CIS QDs upon the addition of [+] MB molecules, thereby confirming the absence any quenching. This can be attributed to the strong electrostatic repulsion which prevents the donor and acceptor moieties from coming close to each other. Hence, it can be confirmed that electrostatics does indeed play a major role in the PL quenching processes in charged CIS QDs.

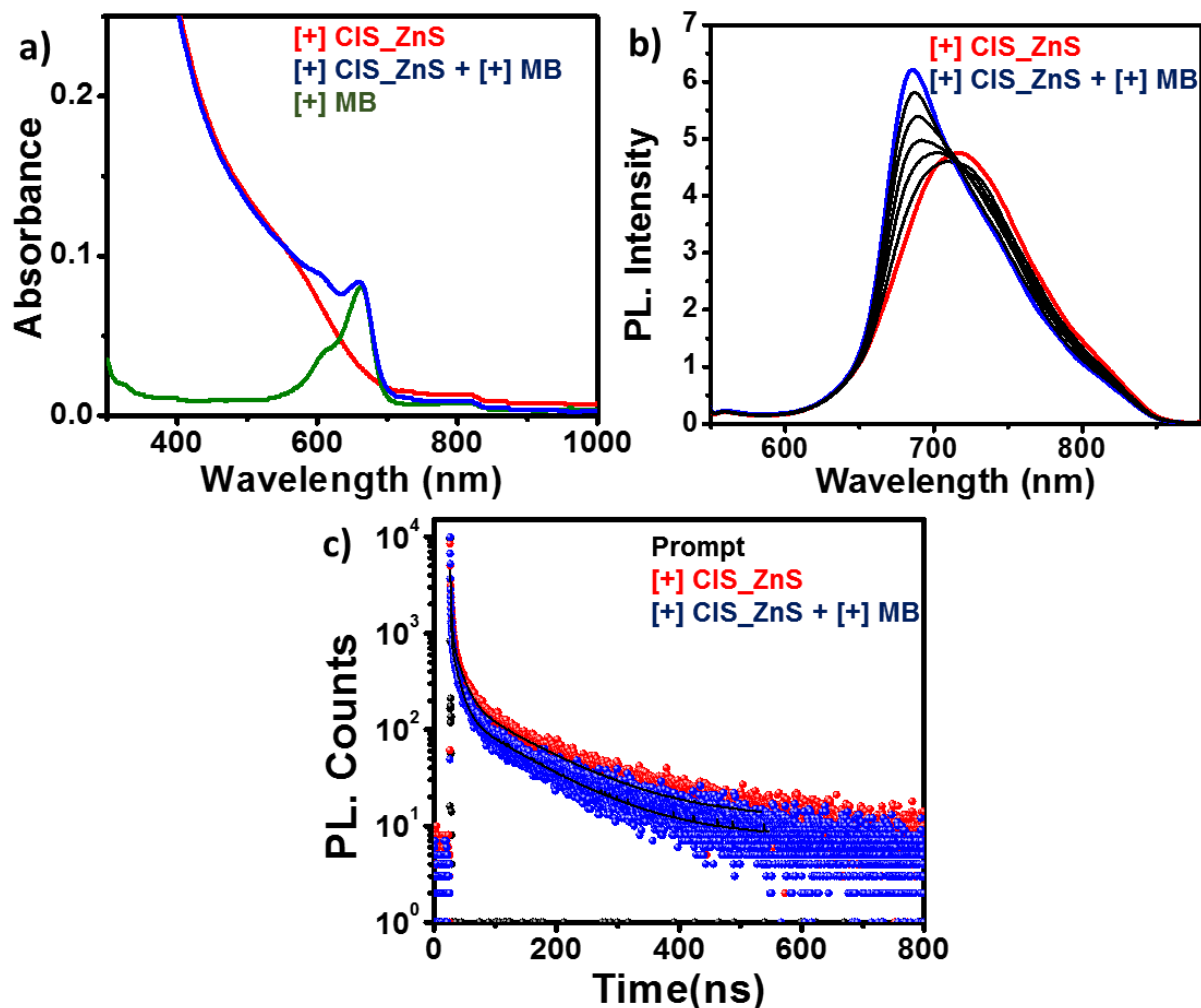


**Figure 4.13: Exclusivity of electrostatic effect in PL quenching in [-] CIS QD – [+] MB nanohybrid. (a)** The absorption spectra of [+] MB dye in the absence and presence of [-] CIS QDs. **(b)** Spectral changes in the PL emission of [-] CIS QDs upon sequential addition of [+] MB dye. **(c)** PL decay profile of [-] CIS QDs in the absence and presence of [+] MB dye, collected at the donor emission of 680nm.

## 5. Conclusions and future direction

The present study provides deeper insights into the fundamental photophysical processes occurring between CIS QDs and organic dye molecules in aqueous medium. We were successful in establishing a protocol for the surface functionalization of CIS QDs, yielding a charged and water-soluble CIS QDs with ~60% retention of the PL QY. The ability of surface engineered CIS QDs to participate as efficient donors in light harvesting processes was systematically investigated. Both the steady state and time resolved studies confirmed an efficient PL quenching of CIS QDs in the presence of ICG dye molecules. PL quenching efficiency as high as ~85% was observed, in aqueous medium, with [+] CIS QDs as the donor and [-] ICG dye as the acceptor. Detailed studies carried out under various conditions (such as oxygen vs inert atmosphere, solvent polarity and temperature dependence) helped in ascertaining the role of electron transfer process as the main mechanism of PL quenching in [+] CIS QD – [-] ICG nanohybrid system. The strong electrostatic attraction between [+] CIS QD and [-] ICG dye was responsible for the formation of a strong ground state complex, which was decisive in achieving an efficient electron transfer in aqueous medium. The exclusivity of electrostatic effect on electron transfer process was proved by extending the PL quenching studies to [-] CIS QD– [+] MB dye nanohybrid system. Successful demonstration of efficient electron transfer process in aqueous medium will expand the use of ecofriendly CIS QDs beyond optoelectronic devices, especially in biomedical applications like sensing, targeting, imaging and so on.



## References

- (1) Wasielewski, M. R. Photoinduced Electron Transfer in Supramolecular Systems for Artificial Photosynthesis. *Chem. Rev.* **1992**, *92*, 435–461.
- (2) Ishizaki, A.; Calhoun, T. R.; Schlau-Cohen, G. S.; Fleming, G. R. Quantum Coherence and Its Interplay with Protein Environments in Photosynthetic Electronic Energy Transfer. *Phys. Chem. Chem. Phys.* **2010**, *12*, 7319-7365.
- (3) Sapsford, K. E.; Berti, L.; Medintz, I. L. Materials for Fluorescence Resonance Energy Transfer Analysis: Beyond Traditional Donor-Acceptor Combinations. *Angew. Chemie - Int. Ed.* **2006**, *45*, 4562–4588.
- (4) Eichelbaum, M.; Rademann, K. Plasmonic Enhancement or Energy Transfer? On the Luminescence of Gold-, Silver-, and Lanthanide-Doped Silicate Glasses and Its Potential for Light-Emitting Devices. *Adv. Funct. Mater.* **2009**, *19*, 2045–2052.
- (5) Stryer, L. Fluorescence Energy Transfer as a Spectroscopic Ruler. *Annu. Rev. Biochem.* **1978**, *47*, 819–846.
- (6) Tvrdy, K.; Frantsuzov, P. A.; Kamat, P. V. Photoinduced Electron Transfer from Semiconductor Quantum Dots to Metal Oxide Nanoparticles. *Proc. Natl. Acad. Sci.* **2011**, *108*, 29–34.
- (7) Plass, R.; Pelet, S.; Krueger, J.; Grätzel, M.; Bach, U. Quantum Dot Sensitization of Organic-Inorganic Hybrid Solar Cells. *J. Phys. Chem. B* **2002**, *106*, 7578–7580.
- (8) Praveen, V. K.; Ranjith, C.; Bandini, E. Assemblies: Versatile Materials for Excitation. *Chem. Soc. Rev.* **2014**, *43*, 4222–4242.
- (9) Bawendi, M. G.; Steigerwald, L. The quantum mechanics of larger semiconductor clusters (“QUANTUM DOTS”). *Annu. Rev. Phys. Chem.* **1990**, *4*, 477–496.
- (10) Chuang, C.-H. M.; Brown, P. R.; Bulović, V.; Bawendi, M. G. Improved Performance and Stability in Quantum Dot Solar Cells through Band Alignment Engineering. *Nat. Mater.* **2014**, *13*, 796–801.
- (11) Bruchez Jr., M. Semiconductor Nanocrystals as Fluorescent Biological Labels. *Science*. **1998**, *281*, 2013–2016.
- (12) Lunz, M.; Gerard, V. A.; Gun'ko, Y. K.; Lesnyak, V.; Gaponik, N.; Susha, A. S.; Rogach, A. L.; Bradley, A. L. Surface Plasmon Enhanced Energy Transfer

- between Donor and Acceptor CdTe Nanocrystal Quantum Dot Monolayers. *Nano Lett.* **2011**, *11*, 3341–3345.
- (13) Clapp, A. R.; Medintz, I. L.; Mauro, J. M.; Fisher, B. R.; Bawendi, M. G.; Mattoussi, H. Fluorescence Resonance Energy Transfer between Quantum Dot Donors and Dye-Labeled Protein Acceptors. *J. Am. Chem. Soc.* **2004**, *126*, 301–310.
- (14) Zhong, H.; Bai, Z.; Zou, B.; Colloidal, I. Tuning the Luminescence Properties of III–Nanocrystals for Optoelectronics and Biotechnology Applications. *Chem Lett* **2012**, *3*, 3167–3175.
- (15) Thomas, A.; Nair, P. V.; Thomas, K. G. InP Quantum Dots: An Environmentally Friendly Material with Resonance Energy Transfer Requisites. *J. Phys. Chem. C* **2014**, *118*, 3838–3845.
- (16) Devatha, G.; Roy, S.; Rao, A.; Mallick, A.; Basu, S.; Pillai, P. P. Electrostatically Driven Resonance Energy Transfer in “cationic” Biocompatible Indium Phosphide Quantum Dots. *Chem. Sci.* **2017**, *8*, 3879–3884.
- (17) Tien, J.; Terfort, A.; Whitesides, G. M. Microfabrication through Electrostatic Self-Assembly. *Langmuir* **1997**, *13*, 5349–5355.
- (18) Deng, D.; Chen, Y.; Cao, J.; Tian, J.; Qian, Z.; Achilefu, S.; Gu, Y. High-Quality CuInS<sub>2</sub>/ZnS Quantum Dots for in Vitro and in Vivo Bioimaging. *Chem. Mater.* **2012**, *24*, 3029–3037.
- (19) Lakowicz, J. R. Principles of Fluorescence Spectroscopy, 3<sup>rd</sup> ed., Springer: New York, **1999**.
- (20) Booth, M.; Brown, A. P.; Evans, S. D.; Critchley, K. Determining the Concentration of CuInS<sub>2</sub> Quantum Dots from the Size-Dependent Molar Extinction Coefficient. *Chem. Mater.* **2012**, *24*, 2064–2070.
- (21) Kaszuba, M.; Corbett, J.; Watson, F. M.; Jones, A. High-Concentration Zeta Potential Measurements Using Light-Scattering Techniques. *Philos. Trans. R. Soc. A Math. Phys. Eng. Sci.* **2010**, *368*, 4439–4451.
- (22) Castro, S. L.; Bailey, S. G.; Raffaele, R. P.; Banger, K. K.; Hepp, A. F. Synthesis and Characterization of Colloidal CuInS<sub>2</sub> Nanoparticles from a Molecular Single-Source Precursor. *J. Phys. Chem. B* **2004**, *108*, 12429–12435.

- (23) Santra, P. K.; Nair, P. V.; George Thomas, K.; Kamat, P. V. CuInS<sub>2</sub>-Sensitized Quantum Dot Solar Cell. Electrophoretic Deposition, Excited-State Dynamics, and Photovoltaic Performance. *J. Phys. Chem. Lett.* **2013**, *4*, 722–729.
- (24) Raphael, E.; Jara, D. H.; Schiavon, M. A. Optimizing Photovoltaic Performance in CuInS<sub>2</sub> and CdS Quantum Dot-Sensitized Solar Cells by Using an Agar-Based Gel Polymer Electrolyte. *RSC Adv.* **2017**, *7*, 6492–6500.
- (25) Lakowicz, J. R.; Weber, G. Quenching of Fluorescence by Oxygen. a Probe for Structural Fluctuations in Macromolecules. *Biochemistry* **1973**, *12*, 4161–4170.
- (26) Kamat, P. V. Photochemistry on Nonreactive and Reactive (Semiconductor) Surfaces. *Chem. Rev.* **1993**, *93*, 267–300.
- (27) Fukuzumi, S.; Ohkubo, K.; Suenobu, T.; Kato, K.; Fujitsuka, M.; Ito, O. Photoalkylation of 10-Alkylacridinium Ion via a Charge-Shift Type of Photoinduced Electron Transfer Controlled by Solvent Polarity. *J. Am. Chem. Soc.* **2001**, *123*, 8459–8467.
- (28) Heitele, H.; Finckh, P.; Weeren, S.; Pöllinger, F.; Michel-Beyerle, M. E. Solvent Polarity Effects on Intramolecular Electron Transfer. 1. Energetic Aspects. *J. Phys. Chem.* **1989**, *93*, 5173–5179.
- (29) Moreira, M. L.; Melo, M. M.; Martins, A. P.; Lyon, P. J.; Romani, P. A.; Codognoto, L.; Santos, C. S.; Oliveira, M. P. Photophysical Properties of Coumarin Compounds in Neat and Binary Solvent Mixtures: Evaluation and Correlation Between Solvatochromism and Solvent Polarity Parameters. *J. Braz. Chem. Soc.* **2014**, *25*, 873–881.
- (30) Venturoli, G.; Drepper, F.; Williams, J. C.; Allen, J. P.; Lin, X.; Mathis, P. Effects of Temperature and Delta G Degrees on Electron Transfer from Cytochrome c(2) to the Photosynthetic Reaction Center of the Purple Bacterium Rhodobacter Sphaeroides. *Biophys. J.* **1998**, *74*, 3226–3240.
- (31) Jortner, J. Temperature Dependent Activation Energy for Electron Transfer between Biological Molecules. *J. Chem. Phys.* **1976**, *64*, 4860–4867.
- (32) Shen, J.-S.; Yu, T.; Xie, J.-W.; Jiang, Y.-B. Photoluminescence of CdTe Nanocrystals Modulated by Methylene Blue and DNA. A Label-Free Luminescent Signaling Nanohybrid Platform. *Phys. Chem.* **2009**, *11*, 5062-5070.

